A DISCUSSION OF UNCERTAINTY QUANTIFICATION FOR CHF AS PERFORMED IN COBRA-IE

D. L. Aumiller and M. J. Meholic
Bettis Atomic Power Laboratory
PO Box 79
West Mifflin, PA 15122 USA
david.aumiller@unnpp.gov; michael.meholic@unnpp.gov

ABSTRACT

An assessment of the predictive capability of COBRA-IE for Critical Heat Flux (CHF) using the 2005 Groeneveld CHF Look-Up Table is presented. The assessment was performed against 13 different open literature CHF experiments which were conducted over a wide range of conditions in various internal flow geometries. Overall, approximately 1300 data points were evaluated.

Different methodologies to quantify the uncertainty inherent in the CHF models are discussed in this paper. The simulation techniques, uncertainty methods, and the results of two of the methods are provided. A discussion of the appropriate use of the various CHF uncertainty methods is included. The results indicate that for the method associated with the largest uncertainty, the average Measured/Predicted value in CHF is 1.19 and the standard deviation is 0.62. For the second method, similar to the critical power ratio used for boiling water reactors, the average ratio is 0.98 and the standard deviation is 0.13. Finally, a method to translate between the various methods is proposed and shown to be accurate. The use of this transformation could permit significant time and cost savings by allowing a single uncertainty assessment to serve two very different analytical needs.

KEYWORDS
COBRA, CHF, critical power, uncertainty, assessment

1. INTRODUCTION

The occurrence and location of CHF is important to the thermal performance of nuclear reactors for both normal operations as well as safety analysis. An assessment of the predictive capability of the COBRA-IE (Coolant Boiling in Rod Arrays – Integrated Environment) for CHF, including an assessment of uncertainty, is reported in this paper. COBRA-IE is a best estimate, three field (vapor/non-condensable gas, continuous liquid, and entrained droplets), subchannel analysis code under development at the Bettis Atomic Power Laboratory. COBRA-IE, a descendent of the COBRA-TF code [1], has been developed as a generic thermal-hydraulic analysis tool that can be applied to many analyses of interest for nuclear reactors such as reactor safety, plant analysis, and steam generator analyses.

This CHF assessment includes approximately 1300 experimental data points and considers data from 13 open literature experiments. These data points cover a wide range of conditions (pressure, mass flux, and hydraulic diameter) in various geometries (tube, annulus, rectangular ducts, and adjacent subchannels). Both upflow and downflow situations as well as uniformly and non-uniformly heated cases are

considered. This assessment examines the performance of the 2005 Groeneveld CHF Look-Up Table (LUT) [2] which has been implemented into COBRA-IE to provide enhanced accuracy relative to the previous COBRA-TF CHF model as described in Reference[1].

2. BACKGROUND

2.1. CHF Mechanisms

The CHF point denotes the boundary between nucleate boiling and transition or film boiling. Nucleate boiling provides a very effective heat transfer mechanism, whereas the heat transfer coefficient is significantly decreased in the transition and film boiling regimes. Thus, post-CHF heat transfer regimes can lead to significantly elevated wall temperatures and cladding failure. In flow boiling, CHF phenomena can be separated into two types: film dryout and departure from nucleate boiling (DNB).

In the dryout case, the liquid film that is normally present on the heated surface is lost and cooling is degraded. There are several competing effects which impact the liquid film thickness: mass transfer due to entrainment and evaporation, both of which are thinning the film, and the deposition of liquid, which is replenishing the liquid film. Eventually, the evaporation of the liquid film will deplete the liquid film resulting in CHF. In the DNB scenario, high intensity, localized nucleate boiling at the heated surface creates a thick bubble layer between the liquid core and the heated surface preventing liquid contact. In this case, a small instability can result in localized vapor blanketing of the heated surface such that cooling is lost and a very rapid temperature excursion begins. Exceeding CHF in either manner results in elevated surface temperatures and increases the potential for fuel damage in a nuclear reactor. Therefore, thermal-hydraulic tools such as COBRA-IE must be able to accurately predict both the power required for the onset of CHF and location of CHF over a wide range of conditions.

2.2. COBRA-IE

COBRA-IE uses a three-field (continuous liquid, vapor, and droplets) formulation to solve multiphase flow problems on a staggered Eulerian-Eulerian mesh using time averaged transient conservation equations for each field. Mechanical non-equilibrium is permitted between the different fields as well as thermal non-equilibrium between the liquid and vapor/gas phases. The hydraulic solution is coupled with the solution of a transient conduction equation to determine the temperature distribution in heat structures.

The COBRA-IE heat transfer package has been improved upon the base heat transfer package in COBRA-TF [3-4] and consists of various mechanistic and empirical heat transfer models and correlations. Appropriate heat transfer coefficients are determined based upon the local fluid conditions and heat structure temperature. This method has been developed to form a continuous boiling curve. Both the CHF and minimum film boiling temperature, T_{min}, are determined based upon empirical models. COBRA-IE then calculates an equivalent heated surface temperature, T_{CHF}, which would exist assuming a nucleate boiling wall heat flux equal to CHF. To complete the boiling curve, COBRA-IE calculates the film boiling heat flux associated with T_{min}. The heated surface temperature is compared to T_{CHF} to determine if pre or post-CHF conditions exist. If the temperature is between T_{min} and T_{CHF}, the transition boiling regime exists; this regime consists of contributions from nucleate and film boiling regimes. It should be noted that COBRA-IE assumes that any continuous liquid film present is uniformly distributed around the periphery of each subchannel. This assumption is adequate for flow in tubes; however, the validity of this assumption for conditions such as single side heating must be established.

COBRA-IE provides a calculation of the Departure from Nucleate Boiling Ratio (DNBR) for all heated surfaces throughout the problem domain. The DNBR is calculated as:

$$DNBR = \begin{cases} \dfrac{q''_{CHF}}{q''_{surf}} & \text{for pre} - \text{CHF conditions} \\ \max\left(0, \left(\dfrac{T_{min} - T_{surf}}{T_{min} - T_{CHF}}\right)^2\right) & \text{for post} - \text{CHF conditions} \end{cases} \quad (1)$$

where q''_{CHF} is the local CHF value, q''_{surf} is the local heated surface heat flux, and T_{surf} is the local heated surface temperature. This method converges to one at the CHF location from either side and is needed since for steady state conditions, the presence of post-CHF flow regimes influences the local, and downstream, CHF values. The post-CHF value provides an indication of the fractional distance into the transition boiling regime. Upon exceeding T_{min} and entering film boiling, the DNBR value is set to zero. The minimum DNBR (or MDNBR value) and location are reported by COBRA-IE over the entirety of the problem domain. This provides an indication of whether CHF has been exceeded at any point in the domain as well the limiting location(s).

COBRA-IE provides numerous CHF model options to the user. In this paper, the accuracy of the 2005 Groeneveld CHF LUT is assessed. The Groeneveld CHF model in COBRA-IE utilizes the 2005 LUT [2] which is formulated as a three-dimensional look-up table. Its independent parameters are pressure, mass flux, and quality. The table values are normalized for uniformly heated tubes with a diameter of 8 mm. Application to other conditions is provided by the use of several correction factors to account for variations in hydraulic diameter, geometry, non-uniform power profiles, and flow direction [7]. It should be noted that the COBRA code series historically calculated the CHF value on a subchannel basis using the local fluid conditions. This CHF value was then applied to all heated surfaces attached to that subchannel. However, one of the correction factors for the Groeneveld LUT depends upon the boiling length. Since different heated surfaces will have different boiling lengths due to differing power levels and axial power shapes, COBRA-IE now calculates a CHF value for each heat structure surface connected to a fluid volume rather than applying a subchannel based CHF value to each surface.

3. UNCERTAINTY METRICS

There are two methods that have historically been used to describe the uncertainty in the critical heat flux calculations. The two methods seek to identify two different parameters; as such, it is important to understand the assumptions that are used in the definition of each such that the decisions regarding the applicability of each for application to Best Estimate Plus Uncertainty (BEPU) methods can be made.

In the first method, the local conditions for an experiment are held constant and the resulting uncertainty in the CHF correlation is determined. This method, called P/M (predicted over measured), can most easily be calculated by determining the inverse, M/P through the use of BEPU analysis tools such as COBRA-IE. This is accomplished by finding the value of M/P that when multiplied by a code predicted CHF value yields the experimentally determined value of CHF.

The second method is more closely related to the Critical Power Ratio (CPR) as used in Boiling Water Reactors. The Critical Power Ratio is defined as "power in the assembly that is calculated of appropriate correlation(s) to cause some point in the assembly to experience boiling transition, divided by the actual assembly operating power" [8]. This method seeks to quantify the uncertainty that is present in the calculation of the power related to CHF vice the uncertainty in the underlying correlation. While the two uncertainty values are related, as will be subsequently shown, they are fundamentally different and should not be used interchangeably. To determine the CPR value, the power for a simulation is increased or decreased from the experimental value until the simulations indicate that the CHF has occurred. The CPR is calculated as the simulation power to achieve CHF divided by the experimental power.

3,1 Relationship between CPR and P/M Uncertainties

It is possible to relate the P/M value and the CPR value for the same case if appropriate assumptions are considered. The most important assumption in the current work is to only consider cases that have a uniform axial power profile. With this assumption, CHF must occur at the exit of the test section. The second assumption is that a one-dimensional energy balance can be performed to determine the appropriate quality at the location of CHF. The final assumption is that a Bowring [9] style CHF correlation, as shown by Equation (2), is valid.

$$q''_{CHF} = \frac{A_{corr} - \frac{D_h G}{4} x h_{fg}}{C_{corr}} \tag{2}$$

where A_{corr} and C_{corr} are correlating parameters and are a function of flow conditions and geometry, x is the local equilibrium quality, D_h is the hydraulic diameter, G is the mass flux, and h_{fg} is the latent heat.

First consider the case where P/M is examined. Dividing Equation (2) by the experimentally determined CHF value (q''_{EXP}) and by writing P/M in terms of the relative P/M error (β), yields:

$$\frac{q''_{Corr}}{q''_{EXP}} = \frac{P}{M} = (1+\beta) = \frac{A_{corr} - \frac{D_h G}{4} x h_{fg}}{C_{corr}\, q''_{EXP}} \tag{3}$$

Performing an energy balance to determine the exit quality at the experimental power in terms of the mass flux, inlet enthalpy (h_{in}), saturated liquid enthalpy (h_f), heat transfer area (A_{HT}) and flow area (A_{flow}) yields the following relationship.

$$A_{corr} + \frac{D_h G}{4}\left(h_f - h_{in}\right) = q''_{EXP}\left\{(1+\beta)C_{corr} + \frac{D_h A_{HT}}{4\, A_{flow}}\right\} \tag{4}$$

Turning our attention to the CPR method, with the definition of CHF from Equation (2) and performing an energy balance where the power is increased yields:

$$q''_{CPR} C_{corr} = A_{corr} + \frac{D_h G}{4}\left(h_f - h_{in}\right) - q''_{CPR}\frac{D_h A_{HT}}{4\, A_{flow}} \tag{5}$$

Substituting Equation (4) into Equation (5), simplifying solving for q''_{CPR}:

$$q''_{CPR} = q''_{EXP}\left\{1 + \beta\left(\frac{1}{1 + \frac{D_h A_{HT}}{4\, A_{flow} C_{corr}}}\right)\right\} \tag{6}$$

Now expressing the error in CPR as relative error (α) provides the following expression between the relative error in P/M and the relative error in CPR.

$$\alpha = \beta\left(\frac{1}{1 + \frac{D_h A_{HT}}{4\, A_{flow} C_{corr}}}\right) \tag{7}$$

Examining Equation (7) reveals that since all of the terms in the parentheses are positive, the relative error in CHF predictions using a critical power ratio approach will always be smaller than the relative error when considered as a multiplier. Furthermore, Equation (7) suggests that it is possible to translate between the two methods using flow parameters.

A discussion concerning when each of the uncertainty methods should be applied in the context of BEPU methods is warranted. The use of CPR methods would be most useful when the concern is determining the power level that can be tolerated without experiencing CHF for conditions such as steady-state CHF performance and operational transients where CHF is to be precluded. It is important to understand that in these situations, it would be impossible to propagate the uncertainty through a simulation via modifications on q''_{CHF} with the direct use of the CPR error data, as this is not what is being captured in the CPR calculation. Equation (7) suggests that the errors from the CPR method could be transformed and propagated through a simulation via modification of q''_{CHF}.

The P/M method would be most appropriate in scenarios such as LOCA simulation where the interest is in determining the uncertainty in CHF for the given local conditions. For instance, during the blowdown phase of a LOCA, the local quality in the core is largely driven by the flashing rate of the fluid and not the boiling of the water from the rods. As such, the use critical power ratio related uncertainty metrics for us in LOCA simulations is not appropriate.

4. EXPERIMENTAL DATA CONSIDERED

The experimental data considered in the COBRA-IE CHF assessment is described below. All of the experiments considered were performed in vertically oriented test sections with primarily one-dimensional flow paths. Table I lists the experiments performed with liquid upflow and uniform power shapes. It should be noted that the Oh & Englert test was only heated on one side while the annulus test of Janseen et al. only heated the inner rod. The dog bone geometry simulated by Grenn et al. was intended to model two adjacent subchannels in a rod bundle. Meanwhile, Table II lists the uniformly heated tests with liquid downflow. For the transients of interest to reactor safety, flow reversal can occur within the core region, and therefore, it is important that CHF can be accurately predicted for either flow direction. Lastly, Table III lists the non-uniformly heated, upflow tests considered in the assessment.

Table I. Uniformly Heated, Upflow Tests

Experiment	Reference	Data Pts	Geometry	P (MPa)	G (kg/m^2-s)	D_h (cm)	L/D_h
Lee & Obertelli	10	625	Tube	3.61 - 11.1	406 - 4421	0.56 - 1.14	20 - 359
Weatherhead	11	105	Tube	13.8	325 - 2658	0.77	59.2
Bennett et al.	12	113	Tube	6.89	379 - 4828	1.26	227 - 438
Oh & Englert	13	58	Duct	0.01 - 0.09	31.3 - 110	0.381	160
Mishima & Nishihara	14	16	Duct	0.01	0 - 71.8	0.450	78
Janseen et al.	15	139	Annulus	6.64 - 9.72	1505 - 3092	0.85 - 1.27	58 - 322
Green et al.	16	40	Dog Bone	8.27 - 13.8	335-2839	0.389	313
Total		1096					

Table II. Uniformly Heated, Downflow Tests

Experiment	Reference	Data Pts	Geometry	P (MPa)	G (kg/m^2-s)	D_h (cm)	L/D_h
Lee & Obertelli	10	16	Tube	3.62-4.24	-4055 - -1030	1.08	80.2
Oh & Englert	13	28	Duct	0.02-0.08	-69.6 - -31.7	0.381	160
Mishima & Nishihara	14	18	Duct	0.101	-284 - -7.2	0.450	78
Total		62					

Table III. Non-Uniformly Heated, Upflow Tests

Experiment	Reference	Data Pts	Power Shape	P (MPa)	G (kg/m^2-s)	D_h (cm)	L/D_h
Lee & Obertelli	17	32	2.12 cosine	3.82 – 7.07	990 – 2047	0.973	188
Lee & Obertelli	17	77	4.27 cosine	3.82 – 11.1	990– 2658	0.973	188
Lee & Obertelli	17	23	5.68 cosine	6.82 – 11.1	1003 – 2034	0.973	188
Total		132					

5. ASSESSMENT METHODOLOGY

The predictive capability of the 2005 Groeneveld LUT CHF model in COBRA-IE is assessed against the entirety of the experimental data described in Section 4. As is discussed in Section 3, two methodologies exist to quantify the uncertainty in the CHF predictions. The following subsections describe the methodologies for obtaining the CPR and P/M values utilizing the MDNBR value in COBRA-IE.

5.1. COBRA-IE Modeling

The base COBRA-IE model consists of a single heat structure attached to a fluid channel. The problem is flow forced by applying a flow and enthalpy boundary condition at the inlet and a pressure and enthalpy boundary condition at the outlet. Test facility specific geometries and experimental conditions (e.g., injection flow, power) are substituted into the base input deck as part of the automation scheme described in Section 5.4. The base axial nodalization is set to a control volume length of 102 mm which corresponds to the recommended axial nodalization for COBRA-IE. When the test section length is not a multiple of 102 mm, the additional test section length is lumped into the first node. Timestep size sensitivities were also conducted to ensure the steady-state results were insensitive.

The 2005 Groeneveld CHF LUT model, with several correction factors, is assessed in this paper. The first correction factor applied is the cross section geometry factor (K_1) which accounts for the normalization of the CHF LUT to an 8 mm tube. An exponent of 0.5 is used. Additionally, the heated length factor (K_4), the axial flux distribution factor (K_5), and the vertical low flow factor (K_8) factors are utilized in the assessment. The final form of the Groeneveld CHF value as used is:

$$q''_{CHF,G} = CPM_{CHF} q''_{CHF,LUT}(P,G,x) K_1 K_4 K_5 K_8 \tag{8}$$

where $q''_{CHF,G}$ is the Groeneveld CHF value and $q''_{CHF,LUT}(P,G,x)$ is the Groeneveld CHF LUT value for pressure P, mass flux G, and quality x. The term CPM_{CHF} represents the manner in which uncertainty in the CHF correlation is propagated through COBRA-IE analyses.

5.2. Critical Power Ratio Methodology

For the CPR methodology, a bisection algorithm is used to find the power that results in a MDNBR value of 1.0 ± 0.02. This requires bounding a MDNBR of one at two different power levels, one resulting in pre-CHF conditions and the other resulting in post-CHF conditions. The search for the bounding power levels starts with a simulation at the experimental power level that corresponded to CHF. Upon obtaining a successful COBRA-IE simulation at the experimental power, one bound for the bisection is obtained. Next, based upon if pre or post-CHF conditions were obtained at the first bounding value, the power level is either increased or decreased, respectively, to search for the second bounding power level. When power increases are required, precautions are needed to prevent power to flow mismatches which result in failed COBRA-IE simulations. To prevent film boiling predictions, and associated MDNBR values of 0.0, the minimum film boiling temperature is increased. A confirmatory COBRA-IE run is then made at the critical power to confirm the adequacy of the steady-state solution. In the event of an unsteady solution, the simulation results are not used.

5.3. Predicted to Measured Methodology

For the P/M methodology, the CHF code physics multiplier (CPM_{CHF}) available in COBRA-IE is utilized to modify the CHF value predicted by the selected CHF model. To ensure local fluid conditions that mimic the experiment, the power level from the experimental data is utilized in the COBRA-IE simulation. Similar to the CPR methodology, a bisection scheme is used to find a MDNBR value of 1.0 ± 0.02. In this method, the CHF code physics multiplier is then varied. Upon obtaining the converged value of the CHF code physics multiplier, a confirmatory COBRA-IE run is made with the multiplier where the adequacy of the steady-state solution is confirmed. In the event that the solution has not reached a steady-state, the simulation results are not used. The resulting M/P (CHF code physics multiplier) can then be inverted to determine the P/M for the simulation.

5.4. Automation Scheme

COBRA-IE utilizes automation extensively for verification and assessment as described by Aumiller et al. [18]. The CHF assessment and uncertainty quantification methods are also automated utilizing the **make** utility which has the ability for parallel execution. A COBRA-IE input deck is constructed for each experimental run by utilizing variable substitutions and a base input deck. This allows run specific conditions such as pressure, injection flow rate, and injection temperature to be varied while maintaining consistency amongst the simulations for issues such as timestep size, modeling options and nodalization. Upon building an input deck for a specific experimental run, MATLAB is used to perform the iteration to find the critical power or CHF code physics multiplier that corresponds to a MDNBR of one depending upon which uncertainty quantification methodology is utilized. Since COBRA-IE can only be executed as a transient analysis code, at the completion of each simulation, time averaging is performed over the last five seconds of the transient to obtain the MDNBR. Additionally, the variability in the calculated MDNBR over the time averaging interval is checked to ensure a steady-state solution has been obtained.

6. CRITICAL POWER RATIO RESULTS

Since CHF data is typically presented using the metric of CPR, these results are discussed first and are presented in Table IV for simulations with at least one successful COBRA-IE simulation. From this table, it is clear that COBRA-IE, using the Groeneveld CHF LUT, is capable of accurately calculating the critical power required to achieve CHF. The mean of the 668 successfully completed CPR analyses is a 0.98 with a median value of 0.96. Both of these values indicate a slight bias toward underpredicting the power required to achieve CHF. The standard deviation of the CPR value is 0.13.

It is clear that the automated CPR search algorithm fails to provide a robust method for completing the required simulations. Only slightly more than 50% of the cases are able to find the CPR value. While precautions were made to prevent inappropriate power to flow ratios, the automated process was often unsuccessful in preventing such scenarios and many calculations were terminated based on such concerns. Additionally, instabilities in some of the calculations created a non-monotonic relationship between power and CHF in the COBRA-IE simulations resulting in additional convergence issues. The method has particular issues with both the very low pressure data (P<1bar) and for cases with downflow. The issues associated with the CPR search algorithm will be investigated in the future.

Table IV. Results Using the Critical Power Ratio Method

Reference	Test Geometry	Flow Direction	Axial Power Shape	Pressure (MPa)	Mass Flux (kg/m^2-s)	# of Convg. Cases	# of Convg. Fail	Mean Pow Mult	Median Pow Mult	Standard Deviation
Lee & Obertelli Upflow	tube	up	uniform	3.62 - 11.14	406.87 - 4421.31	431	187	0.94217	0.9625	0.069022
Weatherhead	tube	up	uniform	13.79	325.50 - 2658.21	82	23	0.98471	1.0012	0.090194
Bennett	tube	up	uniform	6.89	2576.84 - 4828.18	6	107	0.98958	0.99375	0.05938
Green et al.	dog bone	up	uniform	8.27 - 13.79	339.06 - 2834.52	31	9	1.0169	1.025	0.039306
Janssen & Kervinen	annulus	up	uniform (inner rod only)	6.78 - 9.71	1518.98 - 3065.08	63	76	1.1879	1.155	0.19461
Oh & Englert Upflow	duct	up	uniform (1-sided)	0.01 - 0.09	27.12 - 108.50	0	58	-	-	-
Mishima & Nishihara Upflow	duct	up	uniform	0.10	40.69 - 67.81	3	13	1.6961	1.691	0.033003
Lee & Obertelli - 2.12	tube	up	cosine, 2.12	4.10 - 7.07	1057.86 - 2047.91	14	18	1.024	1.0375	0.037217
Lee & Obertelli - 4.27	tube	up	cosine, 4.27	3.83 - 11.17	990.05 - 2034.34	26	51	0.94553	0.925	0.060979
Lee & Obertelli - 5.68	tube	up	cosine, 5.68	6.83 - 11.07	1003.61 - 2034.34	8	15	1.0329	1.0227	0.057867
Lee & Obertelli Downflow	tube	down	uniform	3.96 - 4.17	-1030.73	3	13	0.83167	0.83	0.012583
Oh & Englert Downflow	duct	down	uniform (1-sided)	0.02 - 0.09	-67.81 - -27.12	0	28	-	-	-
Mishima & Nishihara Downflow	duct	down	uniform	0.10	-13.56	1	17	0.1468	0.1468	0
All Data	-	-	-	0.10 - 13.79	-1030.73 - 4828.18	668	615	0.97908	0.9625	0.12853

The histogram of the calculated CPR values is presented in Figure 1. From this figure, we can see that the results are relatively tightly bunched around a value of 1.0 with a slight bias toward underprediction as seen in the mean and median. Additionally, it can be seen that the tails on the distribution extend further to the right than the left. Finally, the data are presented as a comparison of predicted CHF power to the experimental power in Figure 2. From this figure, we can see that the most overpredicted cases are associated with the annular test section of Janssen. In this test section, only the inner surface, which represents the fuel rod, is heated. Additionally, none of the simulations of the Oh data, which are also heated on a single side, are able to complete. The inability of COBRA-IE to adequately calculate CHF in these geometries represents an opportunity for future code development efforts.

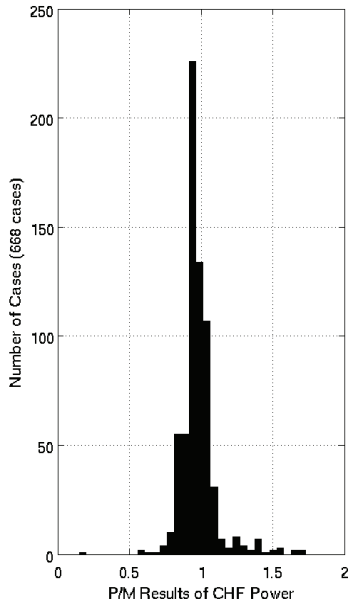

Figure 1. Histogram of Results

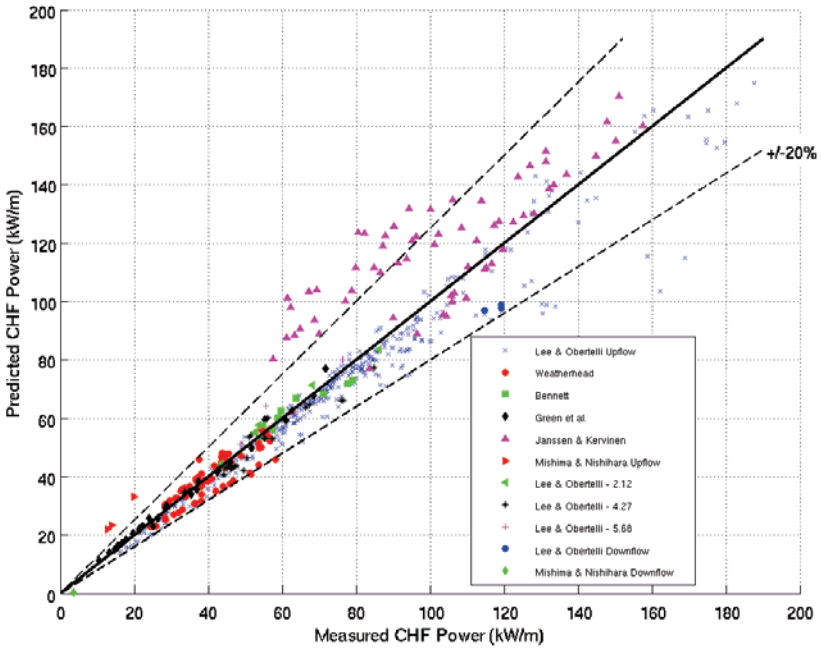

Figure 2. Comparison of Predicted and Measured CHF Powers

Since a wide range of conditions were utilized in the assessments, plots of the results as a function of pressure, mass flux, D_h, L/D_h, and additional solution variables such as local void fraction and quality were generated. The trend plot for system pressure is presented in Figure 2. This figure shows that in spite of the difficulties in obtaining solutions for low pressure cases, there is not a discernible trend in the calculated CPR as a function of pressure. The trend plot for mass flux is presented in Figure 4. This figure shows that downflow cases are characterized by very large scatter in the predicted CPR. The figure shows that combination of COBRA-IE and the Groeneveld CHF correlation has no discernible trend of accuracy in the calculation of CPR with mass flux. The other trend plots, omitted for brevity, indicate no trends of CPR with respect to the parameters investigated.

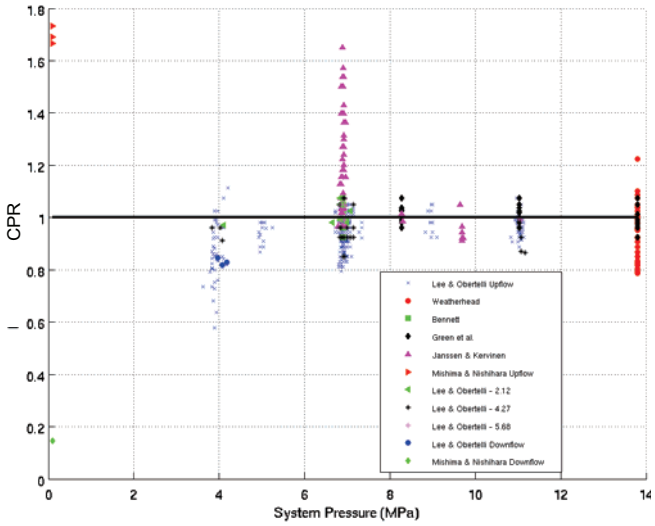

Figure 3. CPR as a Function of Pressure

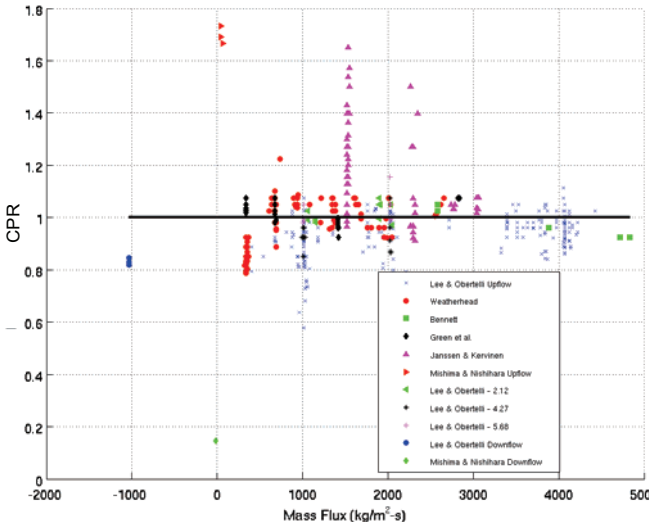

Figure 4. CPR as a Function of Mass Flux

7. M/P RESULTS

Similar results are obtained for M/P method of calculating the accuracy in the CHF calculation. The results are presented in Table V for simulations with at least one successful COBRA-IE simulation. The first obvious difference is in the robustness of this method vice the CPR method. This process returns values for 83% of the simulations. The search algorithm for this uncertainty parameter is noticeably more robust than for the CPR metric. The second observation is that the uncertainty with this method is, as expected, larger than for the CPR method. The mean for M/P is 1.19 and the median is 1.04. The difference between the mean and median indicates that there must be large, asymmetric tails in the distribution of M/P. This is also observed in the fact that the standard deviation for this method is in excess of 60%. The consideration of additional data points shifts the bias in the median from a slight overprediction in CHF to a slight underprediction in CHF. The histogram of the calculated M/P values is presented in Figure 5. From this figure, we can see that the distribution is much wider than for the CPR method. No trends are observed in calculation of M/P for CHF for any of the parameters investigated.

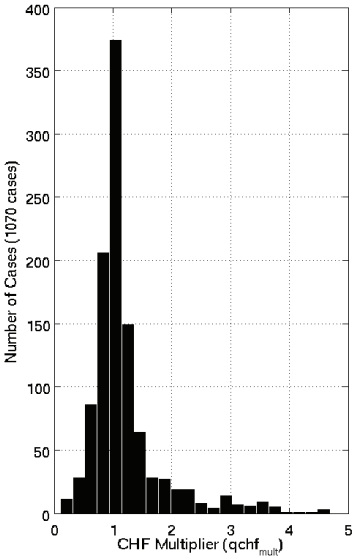

Figure 5. Histogram of M/P as Calculated with COBRA-IE

Table V . Results Using the M/P Method

Reference	Test Geometry	Flow Direction	Axial Power Shape	Pressure (MPa)	Mass Flux (kg/m^2-s)	# of Convg. Cases	# of Convg. Fail	Mean CHF Mult	Median CHF Mult	Standard Deviation
Lee & Obertelli Upflow	tube	up	uniform	3.62 - 11.14	406.87 - 4421.31	542	11	1.4039	1.1439	0.68481
Weatherhead	tube	up	uniform	13.79	325.50 - 2658.21	104	1	1.2052	1.0064	0.53641
Bennett	tube	up	uniform	6.89	637.43 - 4828.18	98	15	0.77702	0.74855	0.17449
Green et al.	dog bone	up	uniform	8.27 - 13.79	339.06 - 2848.08	36	4	0.98441	0.957	0.2627
Janssen & Kervinen	annulus	up	uniform (inner rod only)	6.65 - 9.71	1505.42 - 3092.20	122	7	0.78415	0.80751	0.16517
Oh & Englert Upflow	duct	up	uniform (1-sided)	0.02 - 0.09	27.12 - 108.50	16	42	0.35158	0.35707	0.044683
Mishima & Nishihara Upflow	duct	up	uniform	0.10	13.56 - 67.81	5	11	0.50846	0.41385	0.21292
Lee & Obertelli - 2.12	tube	up	cosine, 2.12	3.83 - 7.07	990.05 - 2047.91	32	0	1.0359	0.94964	0.18915
Lee & Obertelli - 4.27	tube	up	cosine, 4.27	3.83 - 11.24	990.05 - 2658.21	77	0	1.4926	1.2692	0.54951
Lee & Obertelli - 5.68	tube	up	cosine, 5.68	6.83 - 11.10	1003.61 - 2034.34	23	0	0.8859	0.8885	0.097859
Lee & Obertelli Downflow	tube	down	uniform	3.96 - 4.21	-4055.13 - -1030.73	5	11	0.92815	0.8029	0.20405
Oh & Englert Downflow	duct	down	uniform (1-sided)	0.02 - 0.09	-67.81 - -27.12	0	26	-	-	-
Mishima & Nishihara Downflow	duct	down	uniform	0.10	-284.81 - -27.12	10	8	0.18204	0.15002	0.087589
All Data	-	-	-	0.02 - 13.79	-4055.13 - 4828.18	1070	136	1.1931	1.0444	0.62223

8. COMPARISON OF CPR AND M/P UNCERTAINTY

As described in Section 3, it should be possible to relate the uncertainty from the P/M method to the CPR method. To examine the validity of this assertion, the 545 uniform power profile and upflow conditions for which there was both a valid CPR value and a valid M/P case are examined. When focusing on these runs, the mean for the P/M values, obtained by inverting all of the M/P results, is 0.92 while the mean for the CPR is 0.98. This shows that both data sets show a slight bias toward overprediction of CHF. The difference in the standard deviations is significantly larger; the P/M method is 0.31 while the CPR method is 0.12. The histograms for each method are shown in Figure 6. This figure clearly demonstrates that the uncertainty distributions that would be generated from each methodology would be drastically different.

To show that for each of the cases, the error for the CPR method was the lesser of the two, a plot was made comparing the two errors. This plot, shown in Figure 8, clearly shows that with a very few exceptions, which appear in the red regions, the CPR method does provide smaller estimates of error. Additionally, significant scatter is seen in the data and the points appear to have different slopes for the overprediction vice underprediction cases.

To determine if Equation (7) can be used to translate between the two different methods of uncertainty quantification, the C_{corr} parameter from the Bowring correlation, the hydraulic diameter, total heated area and total flow area were used to calculate the right hand side of the equation. This term represents a transformed relative error in the P/M uncertainty method. This value is then compared to the relative error in the CPR method. The results, shown in Figure 8, demonstrate that Equation (7) is an accurate method for translating between the two error methods. Stated another way, if data has already been collected using one of the methods, for the assumptions examined in this paper, it would be possible to generate the second uncertainty distribution without the need to perform a second set of analyses.

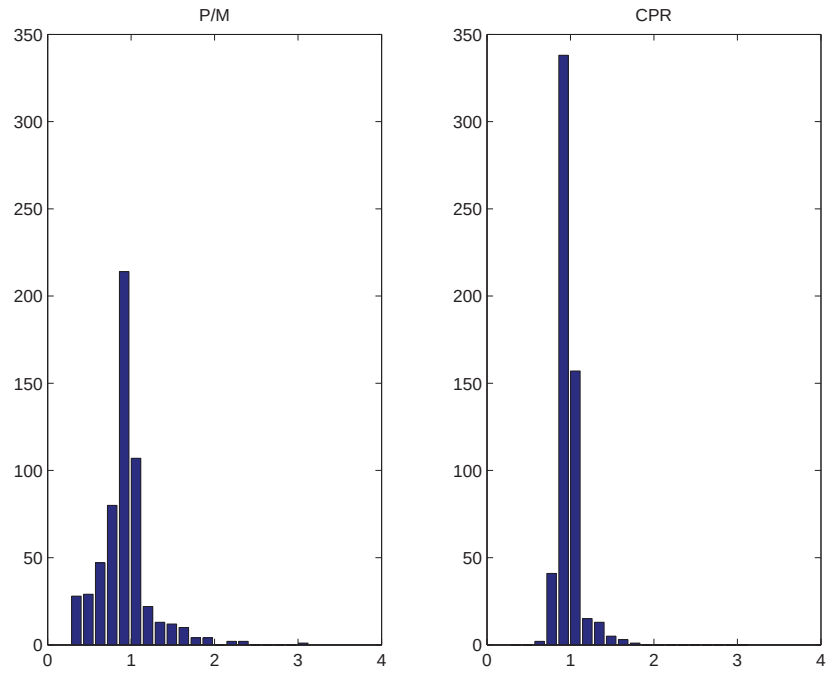

Figure 6. Histograms for Both Uncertainty Quantification Methods for the Same Runs

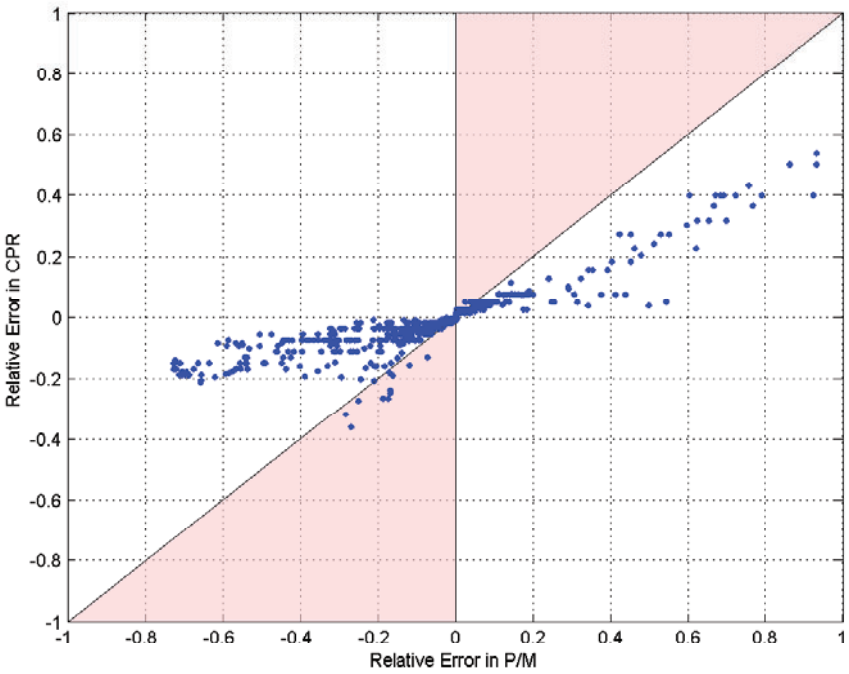

Figure 7. Comparison of Error in CPR and Error in P/M for the Same Runs

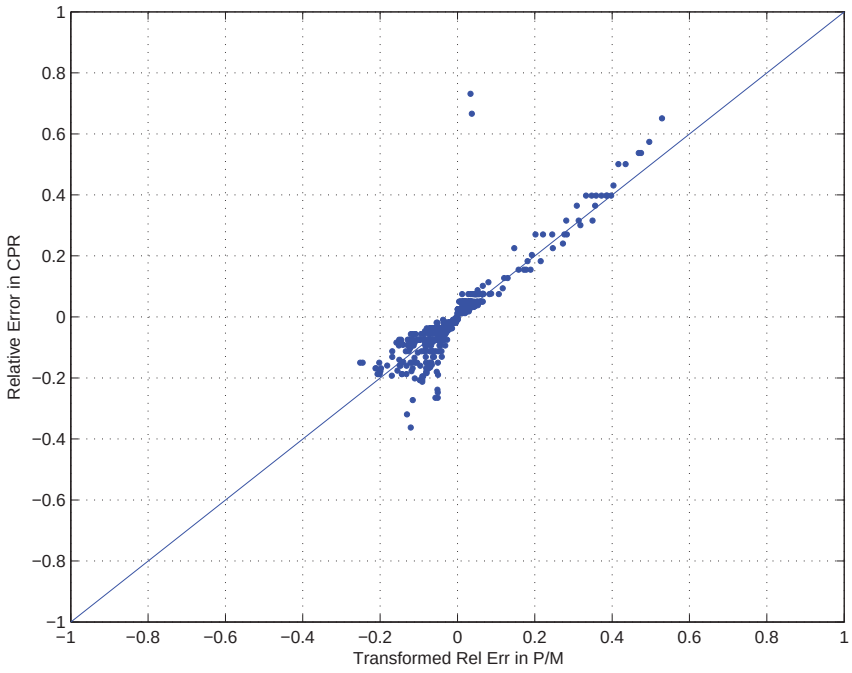

Figure 8. Assessment of Transforming Error in P/M to Error in CPR

9. CONCLUSIONS

The COBRA-IE analysis code has been used to examine CHF in approximately 1300 different CHF data points representing a wide range of geometries, pressures, and mass fluxes. The database is selected to include both upflow, downflow and to include cases with axially varying power shapes. The accuracy of the code is assessed using both the CPR method and with P/M method. The results show that when examined as CPR values, where CHF is impacted by modifying the local quality vice modifying the CHF correlation, the median value was 0.96 and the standard deviation was 0.13. When examined as M/P, the results indicated larger relative errors. A relationship between the two different methods is derived assuming largely one dimensional flow, axially uniform power shapes, and that the Bowring CHF correlation has the correct form. The derivation shows the CPR method will always show a smaller relative error. The adequacy of the derived relationship is validated through the examination of 545 data points for which both methods provide results. The histograms of errors for both cases demonstrate the significant difference between the methods.

The implications of this research are significant. First, it would be entirely inappropriate to use uncertainty distributions that result from calculations of CPR in the context where it is the uncertainty of the CHF correlation is needed, such as for use in LOCA methods employing the BEPU techniques. The second implication is that is appears possible to translate from one method of uncertainty characterization to the other. This would provide the ability to transform CPR data for use as needed.

Future work in this area could examine the effect of removing the assumption of axially uniform power shapes. The theoretical and validation exercises would need to be examined. Finally, this method for transforming error has only focused on the COBRA-IE analysis code. A similar study could be performed with another code to confirm that the method is generically applicable.

REFERENCES

1. M. J. Thurgood, J. M. Kelly, et al., "COBRA/TRAC – A Thermal-Hydraulics Code for Transient Analysis of Nuclear Reactor Vessels and Primary Coolant Systems – Equations and Constitutive Models," *NUREG/CR-3046*, Vol. 1, United States Nuclear Regulatory Commission (1983).
2. D. C. Groeneveld, et al., "The 2005 CHF Lookup Table," *Proceedings of the 11th International Topical Meeting on Nuclear Reactor Thermal-Hydraulics (NURETH-14)*, Avignon, France (2005).
3. M. J. Meholic, "The Development of a Non-Equilibrium Dispersed Flow Film Boiling Heat Transfer Modeling Package," Ph.D. Thesis, The Pennsylvania State University (2011).
4. M. J. Meholic, D. L. Aumiller, and F. Cheung, "A Mechanistic Model for Droplet Deposition Heat Transfer in Dispersed Flow Film Boiling," *Nuclear Technology*, **Vol. 181**, pp. 106-114 (2013).
5. N. Zuber, "On the Stability of Boiling Heat Transfer," *Trans. ASME*, **Vol. 80**, pp. 711 (1958).
6. L. Biasi, et al., "Studeis on Burnout Part 3 – A New Correlation for Round Ducts and Uniform Heating and its Comparison with World Data," *Energia Nucleare*, **Vol. 14**, pp. 535-536 (1967).
7. D. C. Groeneveld, "Lookup Tables for Predicting CHF and Film Boiling Heat Transfer: Past, Present, and Future," *Nuclear Technology*, **Vol. 152**, pp. 87-104 (2005).
8. "Standard Technical Specifications General Electric Plants, BWR/4", *NUREG-1433*, **Vol. 1**, Rev 3 (2004)
9. R. W. Bowring, "A Simple But Accurate Round Tube, Uniform Heat Flux, Dryout Correlation Over the Pressure Range 0.7 – 17 MN/m^2 (100-2500 psia)", Report AEEW-R-789, (1972).
10. J. D. Obertelli and D. H. Lee, "An Experimental Investigation of Forced Convection Burnout in High Pressure Water. Part I. Round Tubes with Uniform Flux Distribution," *AEEW-R-213* (1963).
11. R. J. Weatherhead, "Nucleate Boiling Characteristics and the Critical Heat Flux Occurrence in Subcooled Axial Flow Water Systems," *Argonne National Laboratory*, ANL-6675 (1963).
12. A. W. Bennett et al., "Heat Transfer to Steam Water Mixtures Flowing in Uniformly Heated Tubes in Which the Critical Heat Flux Has Been Exceeded," *United Kingdom Atomic Energy Authority*, AERE-R5373 (1967).
13. C. H. Oh and S. B. Englert, "ATR Critical Heat Flux Experiments Under Low Pressure and Low Flow Conditions," PG-T-91-004, EG&G Idaho (1992).
14. K. Mishima and H. Nishihara, "The Effect of Flow Direction and Magnitude on CHF for Low Pressure Water in Thin Rectangular Channels," *Nuclear Engineering and Design*, **Vol. 86**, pp. 165-181 (1985).
15. E. Janseen et al., "Burnout Conditions for Single Rod in Annular Geometry, Water at 600 to 1400 psia," *United States Atomic Energy Commission*, GEAP-3899 (1963).
16. S. J. Green et al., "Critical Heat Flux on a Coolant Channel Simulating a Closely Spaced Lattice of Rods," *Bettis Atomic Power Laboratory*, WAPD-TM-466 (1969).
17. J. D. Obertelli and D. H. Lee, "An Experimental Investigation of Forced Convection Burnout in High Pressure Water. Part II. Preliminary Results for Round Tubes with Non-Uniform Axial Heat Flux Distribution," *AEEW-R-309* (1964).
18. D.L. Aumiller, et al, "Development of Verification Testing Capabilities for Safety Codes", *Proceedings of NURETH-15*, Paper NURETH15-145, Pisa, Italy (2013).